Electronic Supplementary Material

Coaxial fiber organic electrochemical transistor with high transconductance

Yuan Fang[1], Jianyou Feng[1], Xiang Shi[1], Yiqing Yang[1], Jiajia Wang[1], Xiao Sun[1], Wenjun Li[1], Xuemei Sun[1] (✉), and

Huisheng Peng[1] (✉)

[1] *State Key Laboratory of Molecular Engineering of Polymers, Department of Macromolecular Science, and Laboratory of Advanced Materials, Fudan University, Shanghai 200438, China*

Supporting information to https://doi.org/10.1007/s12274-023-5722-y

Address correspondence to Xuemei Sun, sunxm@fudan.edu.cn; Huisheng Peng, penghs@fudan.edu.cn

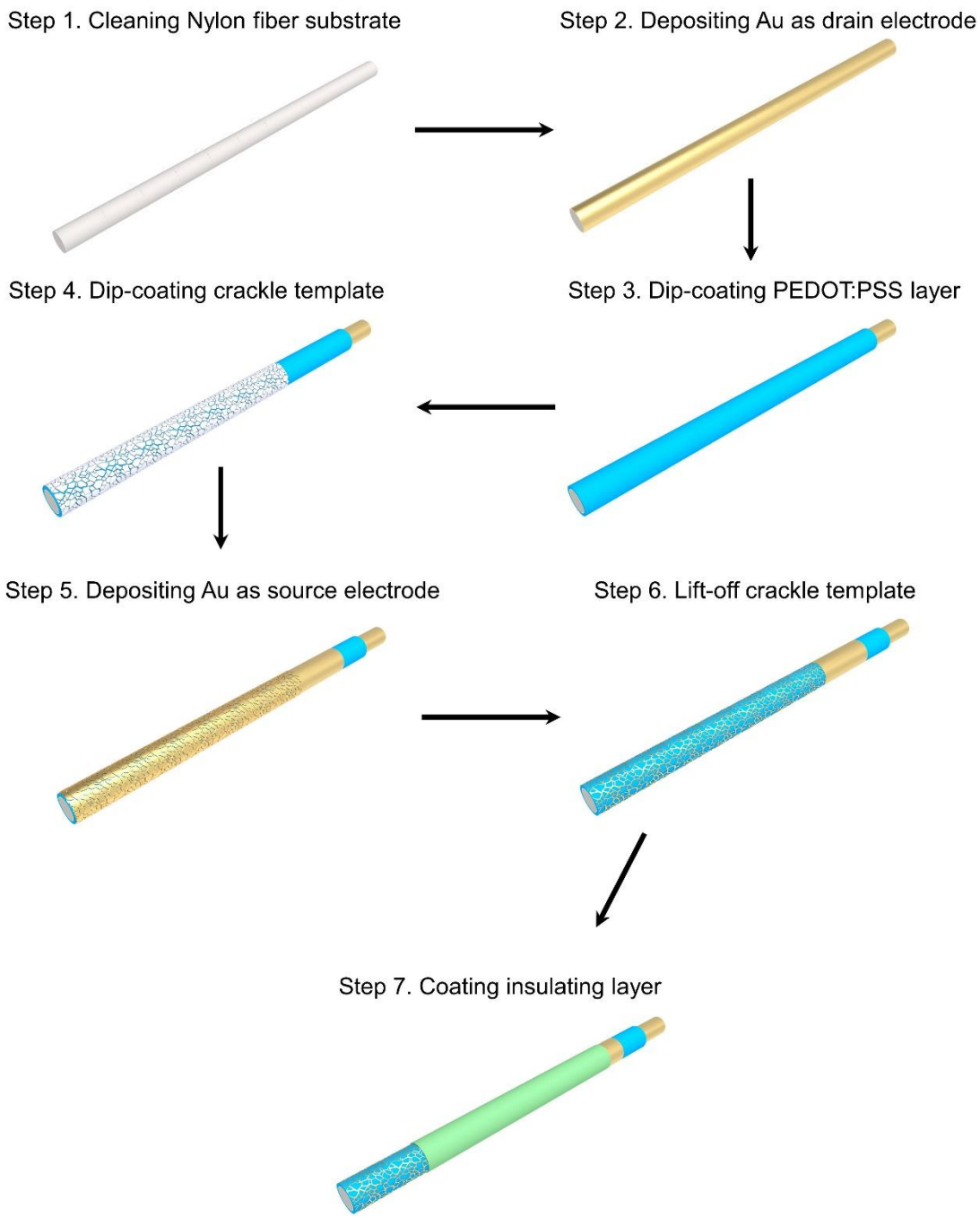

Figure S1 Schematic illustration for the fabrication process of the channel of the coaxial fiber OECT.

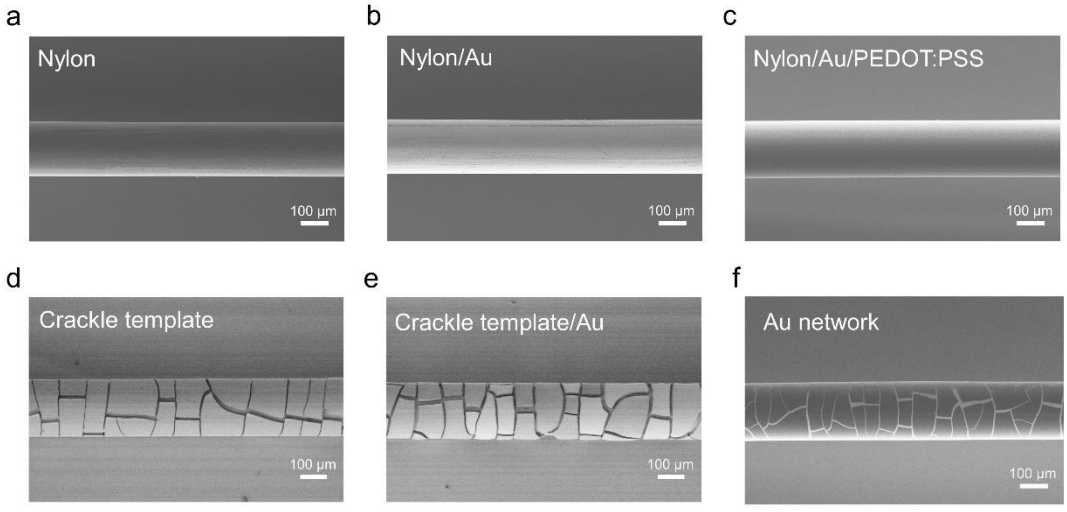

Figure S2 SEM images for the fabrication process of the channel of the coaxial fiber OECT. (a) SEM image of pure nylon fiber. (b) SEM image of nylon fiber coated with 5nm Cr and 100 nm Au layer. (c) SEM image of nylon fiber with Au/PEDOT:PSS coating. (d) SEM image of PEDOT:PSS/Au/nylon fiber deposited with crackle template. (e) SEM image of crackle template deposited with 50 nm Au. (f) SEM image of Au network on PEDOT:PSS layer after lift-off.

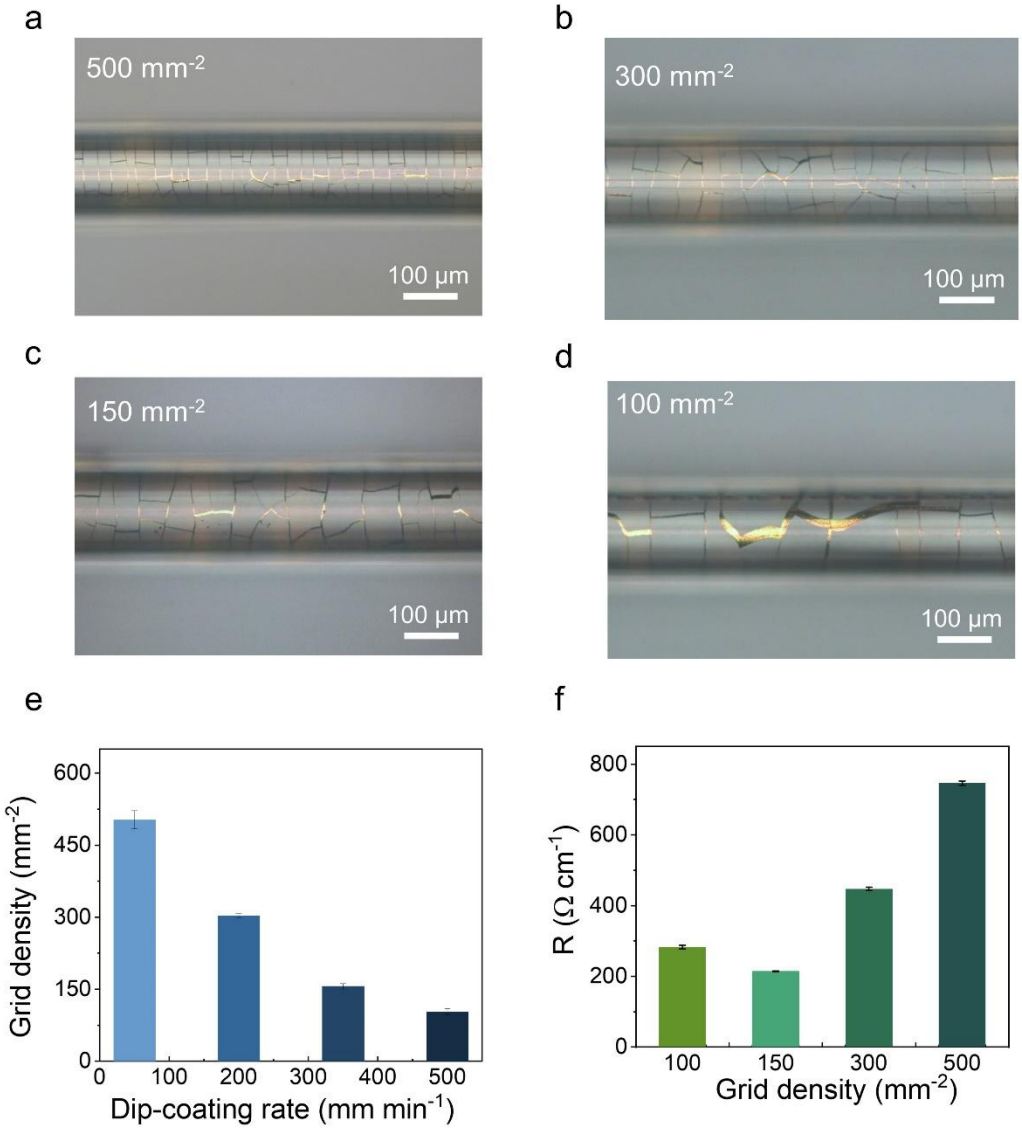

Figure S3 Optical microscopy images for the Au network with different grid densities including (a) 500 mm^{-2}, (b) 300 mm^{-2}, (c) 150 mm^{-2} and (d) 100 mm^{-2}. (e) Grid density using different dip-coating rates. (f) Resistance of Au network with different grid densities.

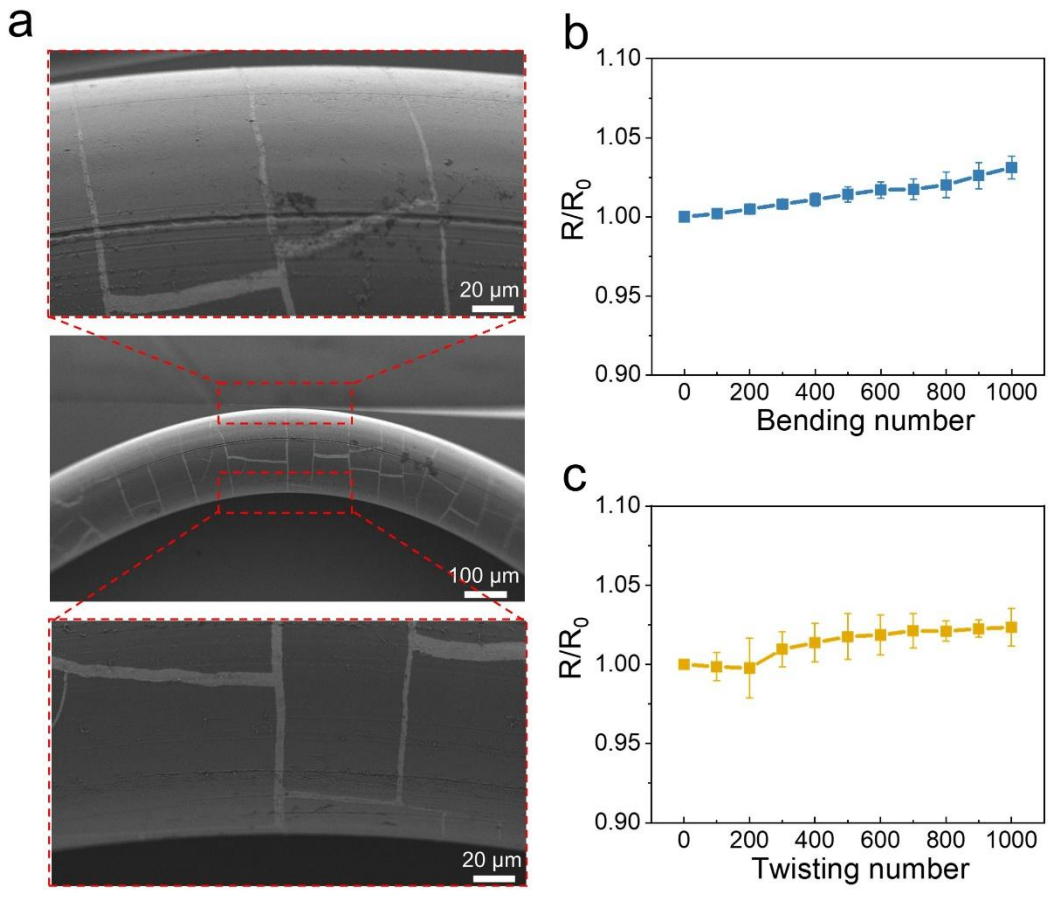

Figure S4 Bending and twisting stability of Au network electrodes. (a) SEM images of Au network electrode under bending. (b) Normalized resistance under bending for 1000 times with a bending radius of 0.5 mm. (c) Normalized resistance under twisting for 1000 times with a twisting angle of 90 °.

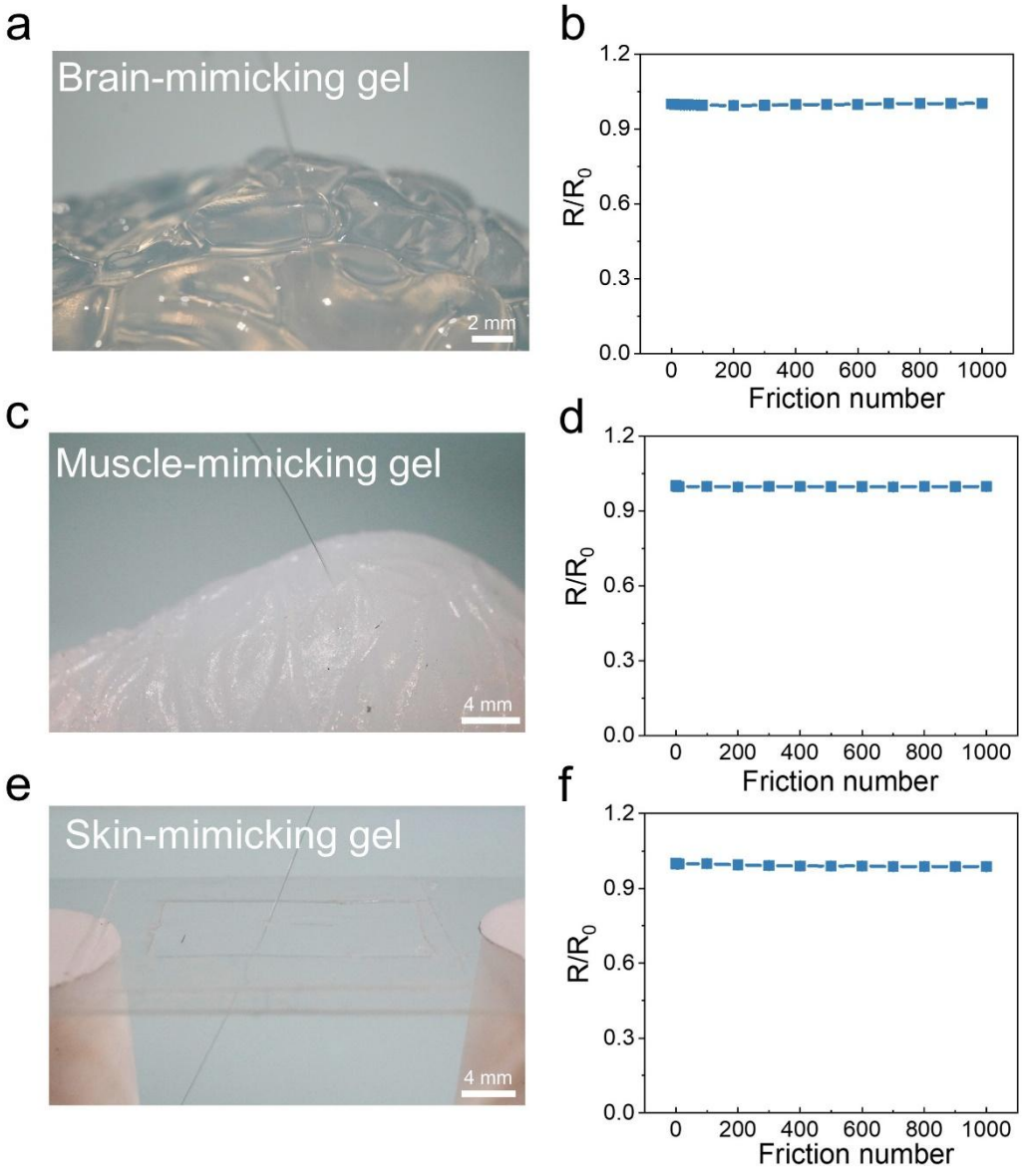

Figure S5 Friction stability of Au network electrodes under different moduli. (a, b) Photographs and normalized resistance of electrodes rubbing against 0.6% agarose hydrogel mimicking brain for 1000 times; (c, d) Photographs and normalized resistance of electrodes rubbing against 2% agarose hydrogel mimicking muscle for 1000 times; (e, f) Photographs and normalized resistance of electrodes rubbing against 3% agarose hydrogel mimicking skin for 1000 times.

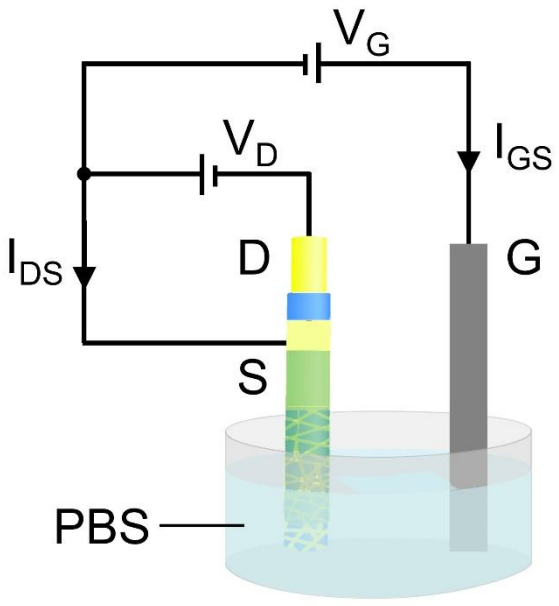

Figure S6 The electrical circuit diagram of the coaxial fiber OECT in PBS solution.

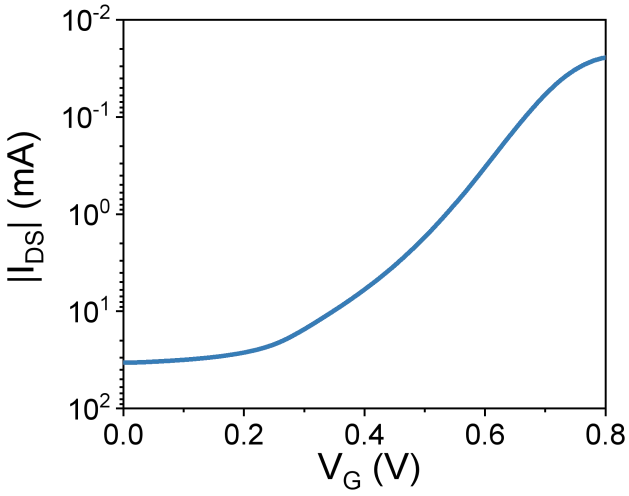

Figure S7 Transfer curve in the logarithmic scale used to calculate the on-off current ratio. The drain current drops from 34 mA at V_G=0 V, to 24 μA at V_G=0.8 V.

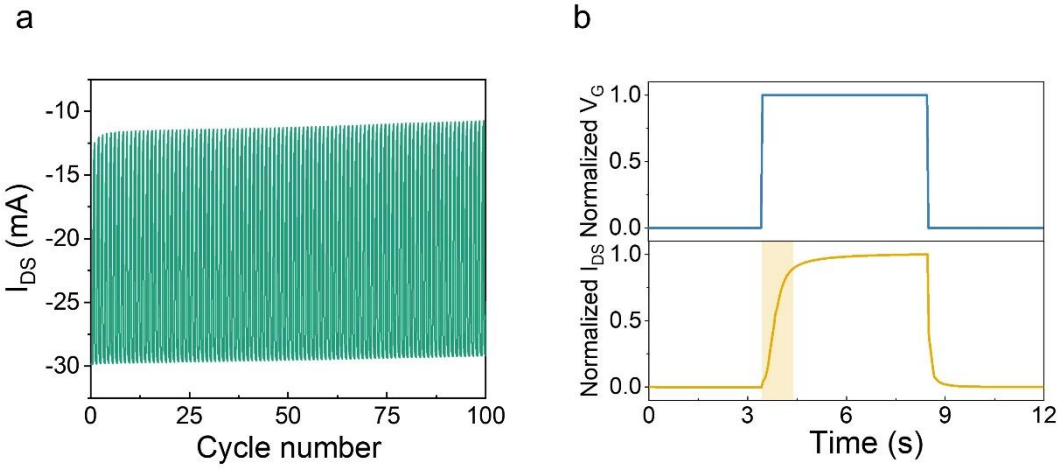

Figure S8 (a) The operational stability of coaxial fiber OECT upon V_G switching from 0 to 0.3 V for 100 cycles. (b) Normalized drain current response to the normalized pulse voltage applied to the gate. The yellow rectangular shadow represents the response time of 0.85 s.

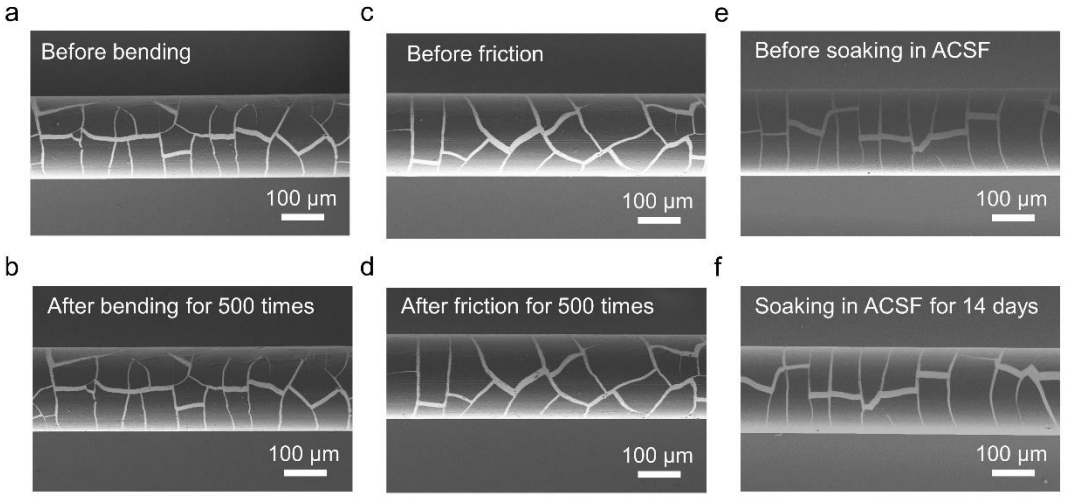

Figure S9 SEM images for stability characterization of coaxial fiber OECTs. (a) Before bending. (b) After bending 500 times. (c) Before friction. (d) After friction 500 times. (e) Before soaking in ACSF. (f) After soaking in ACSF for 14 days.

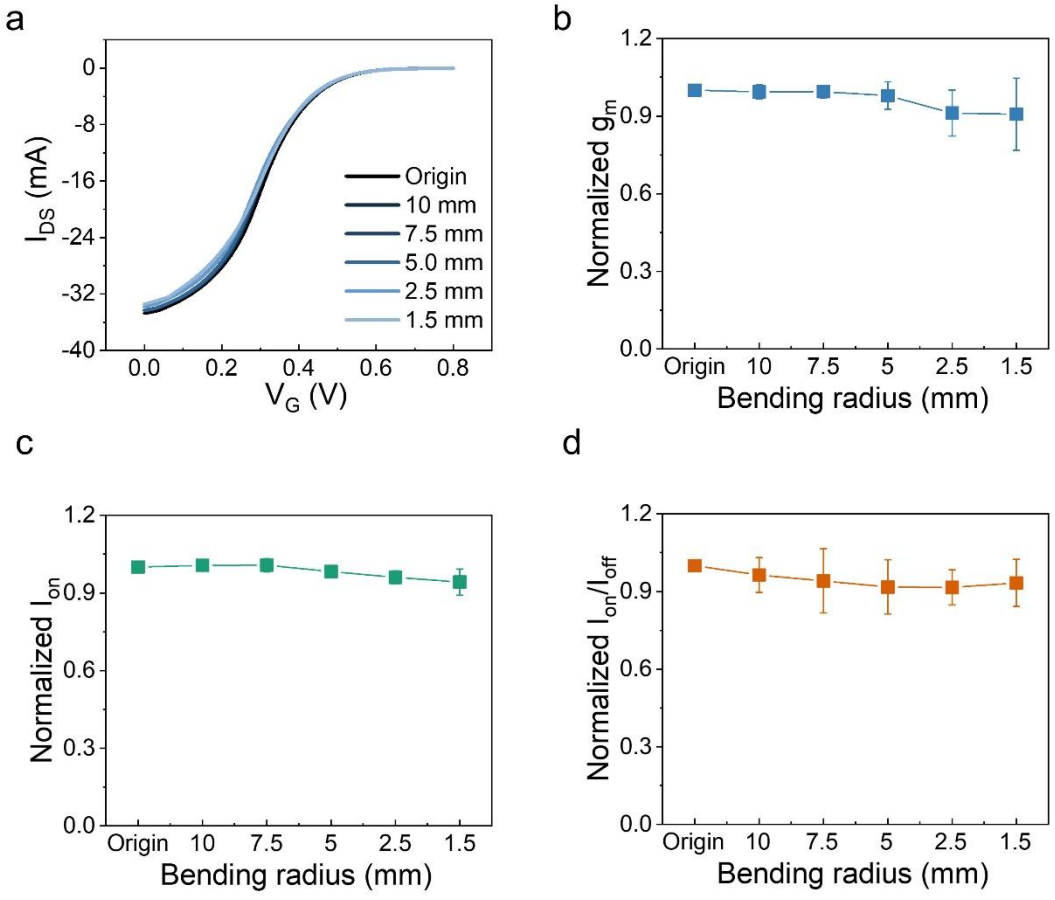

Figure S10 Bending stability under different bending radii. (a) Transfer curves. (b) Normalized transconductance. (c) Normalized on-state current. (d) Normalized on-off current ratio.

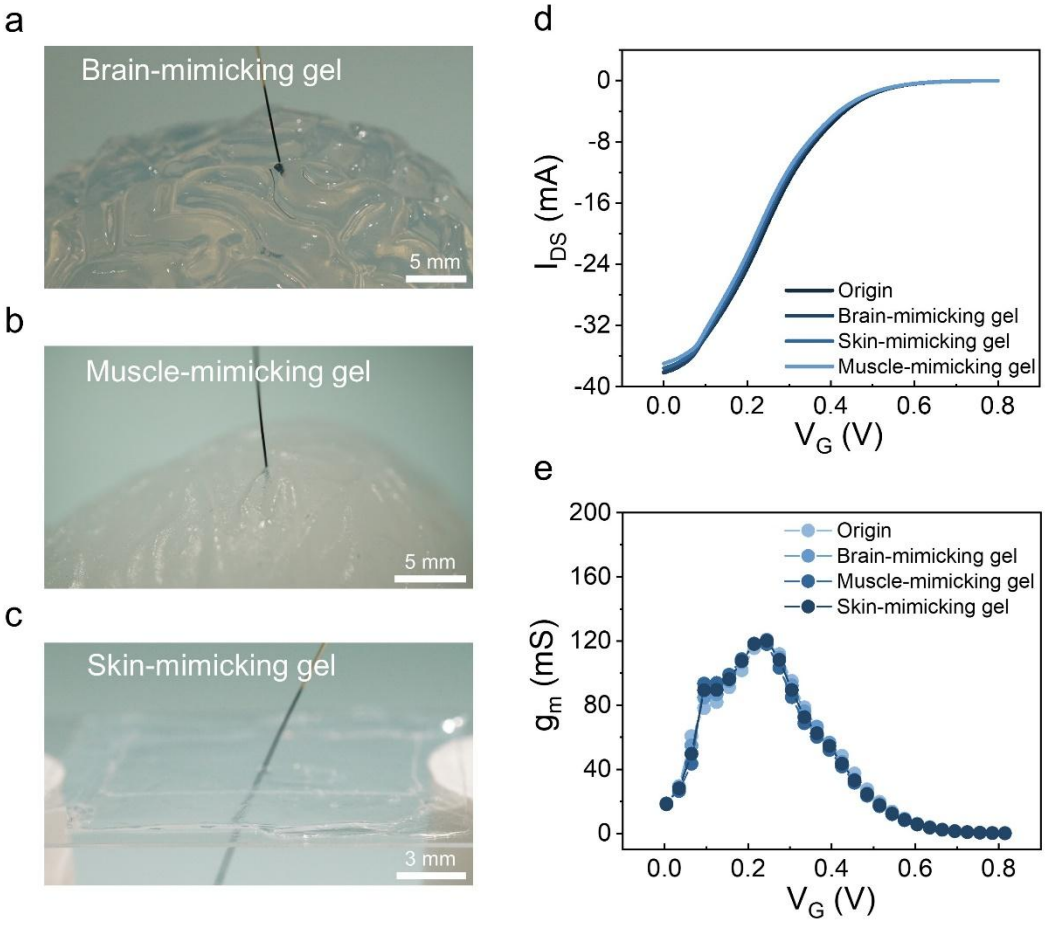

Figure S11 Friction stability of coaxial fiber OECTs under different moduli. Photographs of coaxial fiber OECTs rubbing against (a) brain-mimicking gel composed of 0.6% agarose; (b) muscle-mimicking gel composed of 2% agarose; (c) skin-mimicking gel composed of 3% agarose. (d, e) Transfer curves and transconductance curves under different friction moduli.

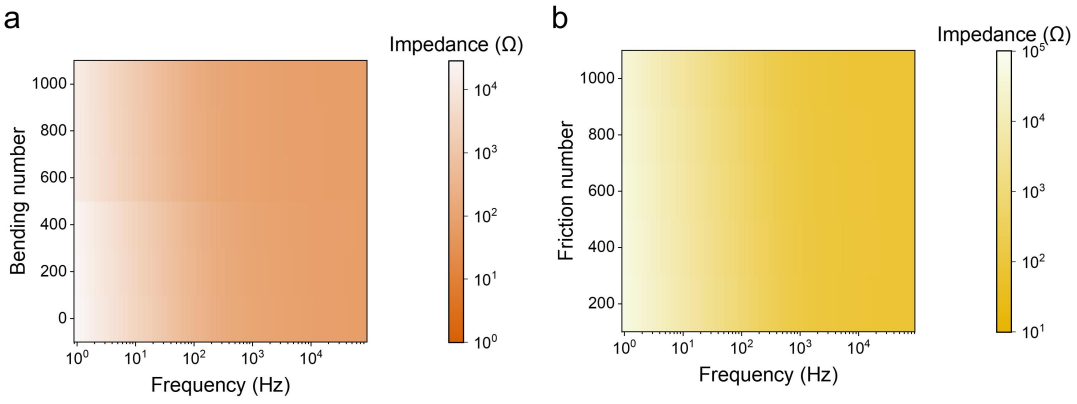

Figure S12 (a, b) The impedance of CNT fiber gate electrode under 1000 bending times and 1000 friction times.

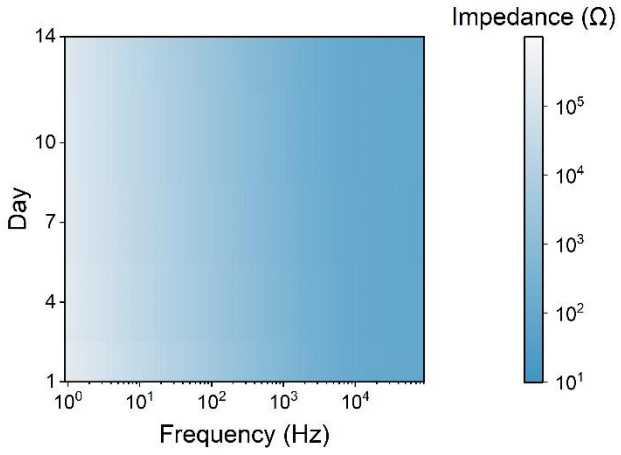

Figure S13 The impedance of CNT fiber gate electrode during 14 days in artificial cerebrospinal fluid.

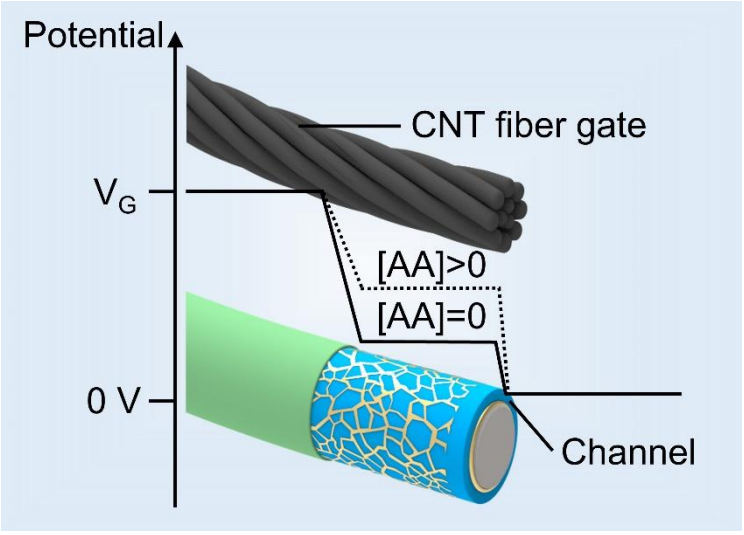

Figure S14 The working mechanism for the coaxial fiber OECT detecting AA.

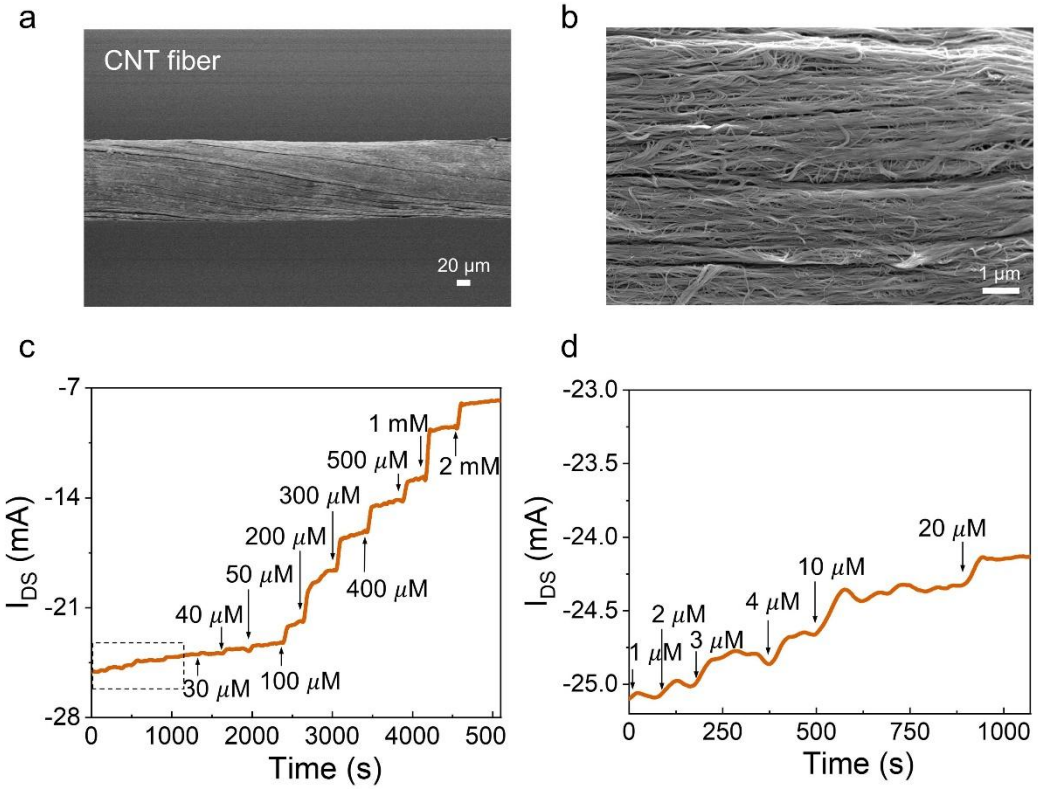

Figure S15 (a, b) SEM images of CNT fiber at low and high magnifications, respectively. (c) Drain current response to the addition of AA with different concentrations. (d) The enlarged view of the dotted box area in figure c represents the response to the concentration of 1-20 μM.

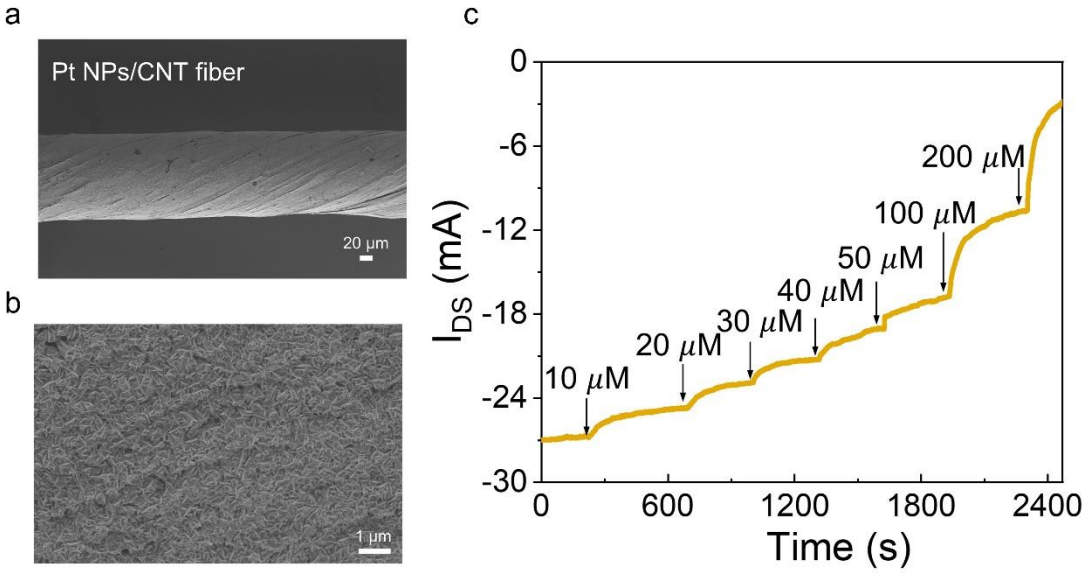

Figure S16 (a, b) SEM images of CNT fiber modified with Pt nanoparticles at low and high magnifications. (c) Drain current responses to the addition of H_2O_2 with different concentrations.

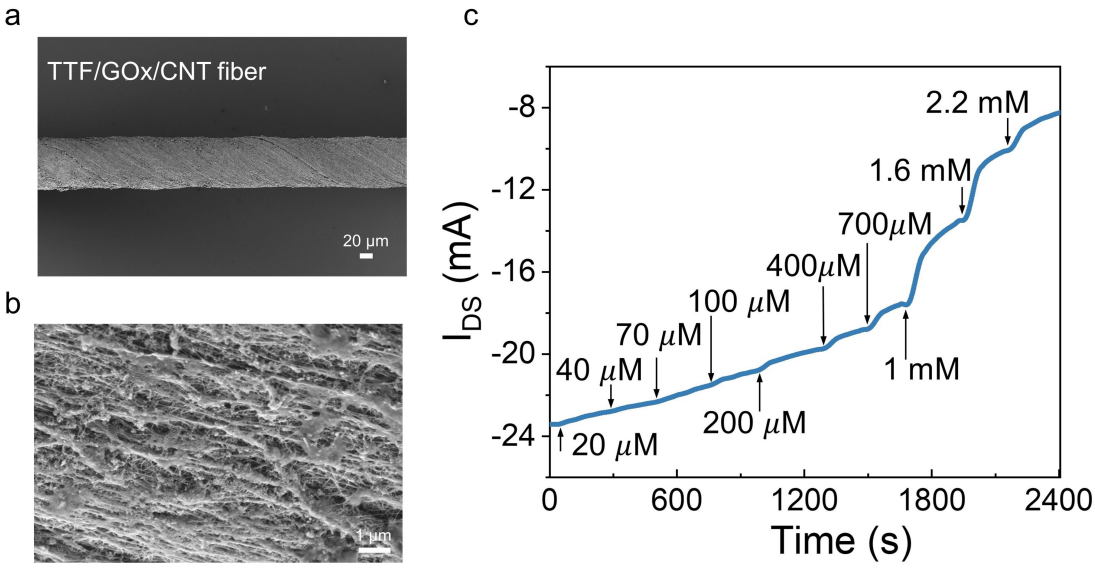

Figure S17 (a, b) SEM images of TTF/GOx/CNT fiber gate electrode at low and high magnifications. (c) Drain current responses to the addition of glucose with different concentrations.

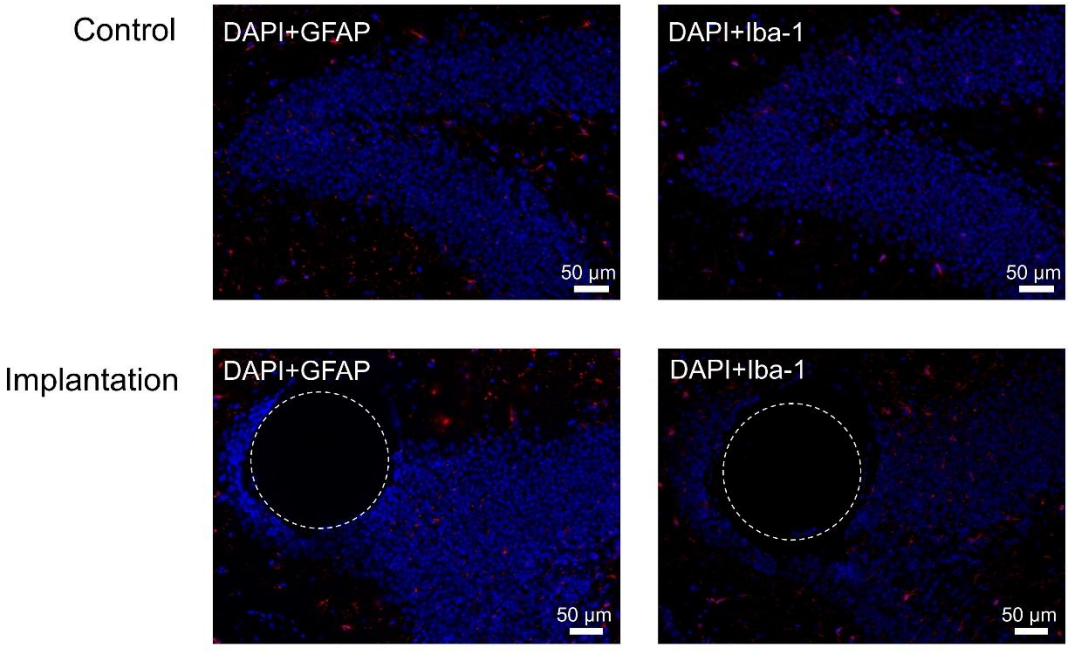

Figure S18 Immunofluorescence images of brain slices with implanted fiber OECTs for 7 days and the control group without implantation. Blue, DAPI, nucleus; red, GFAP and Iba-1, astrocytes and microglia. The white dotted circles indicate the position of fiber OECTs (color online).

Table S1 Comparison of the transconductance and AA sensitivity of this work over that of other OECT based sensors

Transconductance/ (mS)	Sensitivity/ (mA·decade^{-1})	Ref.
135	12.78	This work
2.1	0.62	22
0.23	0.25	39
0.26	0.012	40
0.28	0.061	41
0.23	0.02	42
0.15	0.15	43
0.46	0.075	44
0.12	0.097	45

Table S2 Comparison of the transconductance and H_2O_2 sensitivity of this work over that of other OECT based sensors

Transconductance/ (mS)	Sensitivity/ (mA·decade^{-1})	Ref.
135	20.53	This work
1.35	0.0026	13
0.1	0.037	15
40.1	2.1	30
10	0.24	47
0.35	0.048	48
2	0.07	49
0.52	0.018	50
4	0.48	51

Table S3 Comparison of the transconductance and glucose sensitivity of this work over that of other OECT based sensors

Transconductance/ (mS)	Sensitivity/ (mA·decade^{-1})	Ref.
135	3.78	This work
0.48	0.06	9
0.13	0.03	26
40.1	1.72	30
2	0.069	49
4	0.37	51
2.5	0.88	52
10	1.35	53
16	1.65	54
30	1.91	55
2	0.043	56
1.2	0.077	57
1.1	0.2	58